DALLAS SEMICONDUCTOR MAXIM

Engineering Journal

Volume Three

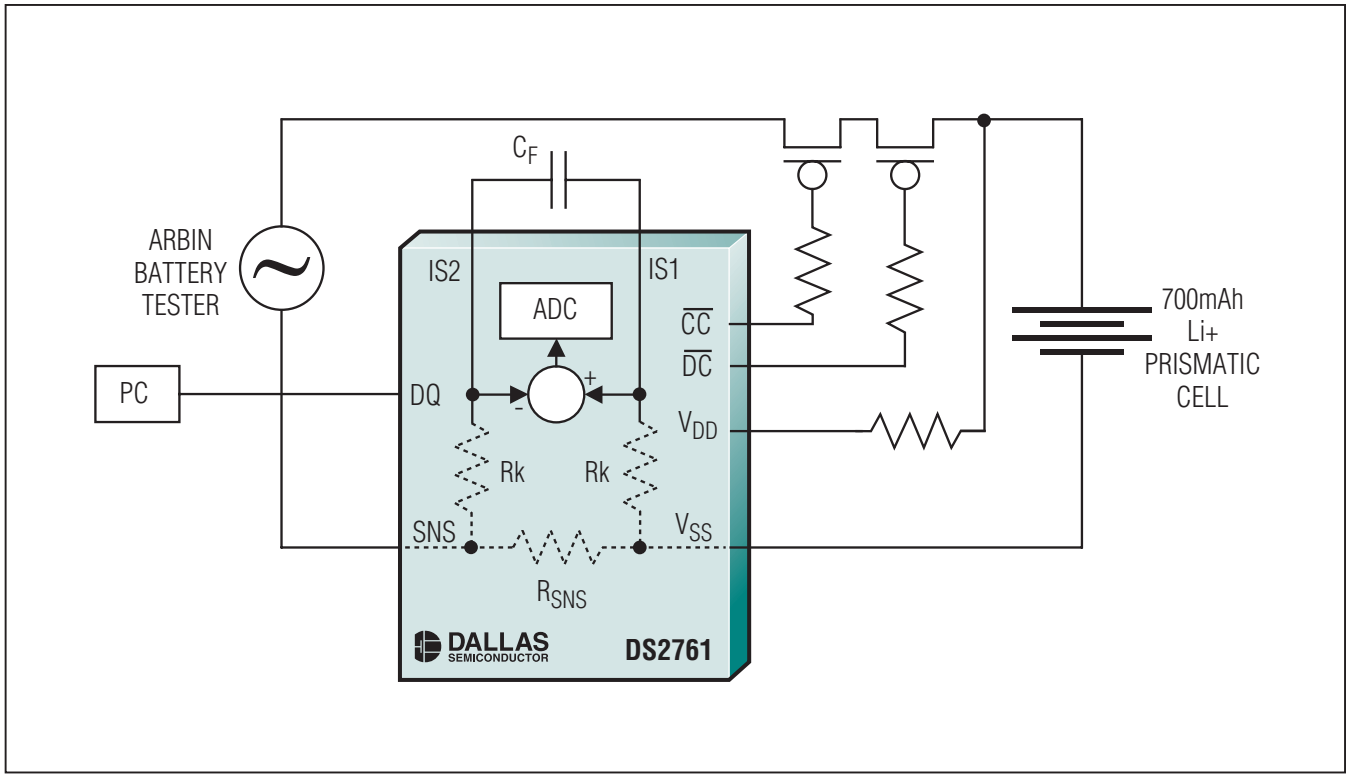

The effectiveness of a discrete-sampled coulomb counter in a pulsed-current application can be demonstrated in the lab using a simulated GSM or CDMA load from an Arbin battery tester.

News Briefs

MAXIM REPORTS REVENUES AND EARNINGS FOR THE THIRD QUARTER OF FISCAL 2002

Maxim Integrated Products, Inc., (MXIM) reported net revenues of $258.5 million for its fiscal third quarter ending March 30, 2002, a decrease from the $397.8 million reported for the third quarter of fiscal 2001 but up from the $247.1 million reported for the second quarter of fiscal 2002. Net income for the quarter was $66.7 million, a decrease from the $109.9 million reported last year but an increase over the $62.6 million reported for the previous quarter. Diluted earnings per share were $0.19 for the third quarter, a decrease from the $0.31 reported for the same period a year ago but up from the $0.18 reported for the second quarter of fiscal 2002.

During the quarter, the Company repurchased approximately 2.7 million shares of its common stock for $141.9 million and acquired a total of $23.1 million of capital equipment. During the fourth quarter of fiscal 2002 to date, the Company has repurchased an additional 3.0 million shares of its common stock for $160.7 million. Accounts receivable increased $13.8 million in the third quarter to $108.6 million, primarily as a result of increased revenues, while inventories decreased $6.7 million to $147.7 million.

Gross margin for the third quarter increased slightly to 70.2%, after increasing inventory reserves $2.1 million, compared to 70.1% reported for the second quarter. Research and development expense increased from the $68.6 million reported in the second quarter or 27.7% of net revenues to $69.0 million or 26.7% of net revenues. Selling, general and administrative expenses decreased from $22.9 million in the second quarter to $22.0 million in the third quarter.

Third quarter bookings were approximately $299 million, a 30% increase over the second quarter's level of $230 million. Turns orders received during the quarter were $140 million, a 12% increase over the $125 million received in the prior quarter (turns orders are customer orders that are for delivery within the same quarter and may result in revenue within the same quarter if the Company has available inventory that matches those orders). Order cancellations remained low for the second consecutive quarter. Bookings increased in all geographic regions and in all but one of the Company's business units.

Third quarter ending backlog shippable within the next 12 months was approximately $219 million, including $195 million requested for shipment in the fourth quarter of fiscal 2002. Second quarter ending backlog shippable within the next 12 months was approximately $187 million, including $170 million requested for shipment in the third quarter of fiscal 2002.

Jack Gifford, Chairman, President, and Chief Executive Officer, commented on the quarter: "Maxim's third quarter was encouraging in many respects. Bookings were up in every geographic region and in all but one of our business units. In addition, cancellations continued to fall to 5% of net bookings in the third quarter. For the first time in six quarters, we have begun to build backlog which, if continued, should improve visibility in future quarters."

Mr. Gifford continued: "Although our outlook for the fiber and telecommunications markets remains conservative, we have seen quarter over quarter bookings growth in the third quarter."

Mr. Gifford concluded: "Based on our estimate of end market consumption of our products, except for fiber and telecommunications equipment, we believe that our customers have worked through their inventories and are ordering for their near-term needs."

Certain statements in this press release are forward-looking statements within the meaning of the Private Securities Litigation Reform Act of 1995. These statements involve risk and uncertainty. They include the Company's expectations as to the consequences of increasing backlog, the Company's assessment of the outlook for the fiber and telecommunications markets, and the Company's assessment of its customers' current ordering activities. Results could differ materially from those forecasted based upon, among other things, the Company incorrectly assessing customer end-user demand and willingness to commit to inventories and orders, and order cancellation levels; technical difficulties in bringing new products and processes to market in a timely manner; market developments that could adversely affect the growth of the mixed-signal analog market such as further declines in customer forecasts or greater than expected cyclical downturns within the mixed-signal analog segment of the semiconductor market or possible effects of capacity constraints affecting other suppliers to equipment manufacturers; and the Company being unable to sustain its successes in recruiting and retaining high-quality personnel and its successes in the markets its products are introduced in, as well as other risks described in the Company's Form 10-K for the fiscal year ended June 30, 2001.

All forward-looking statements included in this news release are made as of the date hereof, based on the information available to the Company as of the date hereof, and the Company assumes no obligation to update any forward-looking statement

Maxim Integrated Products is a leading international supplier of quality analog and mixed-signal products for applications that require real world signal processing.

Interfacing digitally controlled pots and resistors to laser drivers

The different modes of electrical interface between a laser driver and the digitally controlled potentiometers and resistors that control it are reviewed in the context of open- and closed-loop operation. The objective in these fiber-optic systems is to vary the amplitude of light using the laser driver's bias and modulation circuits, causing the optical power to swing between two levels (P0 and P1).

Open-loop topologies

In the bias-control topology of **Figure 1a**, the variable resistor sets a current (I1) that is amplified and fed to a common-cathode laser diode (or sunk from a common-anode type). The most common voltage across the resistor is 1.2V, which is derived from a bandgap reference internal to the laser driver. I1 ranges from microamperes to a few milliamperes, and I2 ranges from tens of milliamps to 100mA. For some applications in which the resistor sources current, it can be connected to a fixed reference or to the supply instead of ground.

Figure 1b shows a low-side circuit (control with respect to ground) in which the input voltage V1 sets an internal current I1, which is amplified to a level of I2 for driving the laser by either sourcing or sinking current. The potentiometer in this circuit is ideal for the high-input impedance seen by V1. (In the Figure 1a configuration, a variable resistor is more appropriate.)

For high-side control **(Figure 1c)**, a decreasing control voltage (V1) causes an increase in I1 and in the laser-drive current I2. Thus, to increase the laser output's average optical power, resistance has to decrease in Figure 1a, V1 has to increase in Figure 1b, and V1 has to decrease in Figure 1c.

Circuit configurations for control of the laser-modulation level (**Figures 2a** and **2b**) are similar to those for control of the bias current. Amplitude modulation of the data carrier produces a switched current. To increase the peak-to-peak amplitude of emitted light, lower the variable resistance in Figure 2a or increase V3 in Figure 2b. (These diagrams show the injection of bias current into the laser as well as modulation current.) In Figure 1b and 2b, note that the input stage of the laser driver IC, which carries I1 or I3, can be a bipolar npn transistor.

Closed-loop topologies

Average power control (APC) is a common means for regulating the average optical output of a laser. The laser is controlled by a photodiode monitor in the feedback path, resulting in closed-loop control of the laser light.

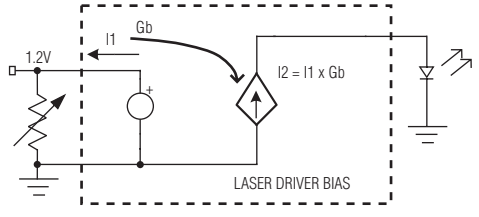

Figure 1a

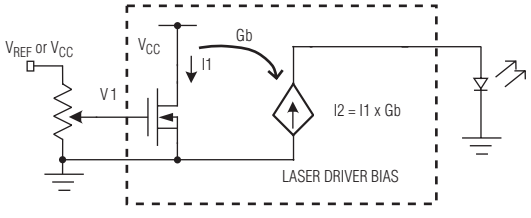

Figure 1b

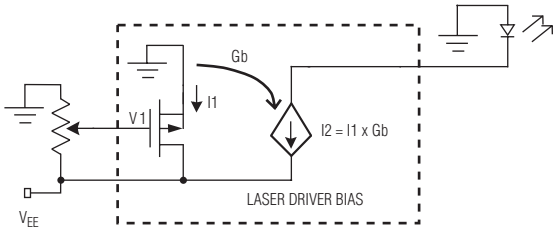

Figure 1c

Figure 1. Open-loop methods for control of laser-bias current include (a) low-side control (laser-cathode grounded) with a variable resistor, or (b) a potentiometer driving a high-impedance input, and (c) high-side control (laser anode grounded) with a negative supply.

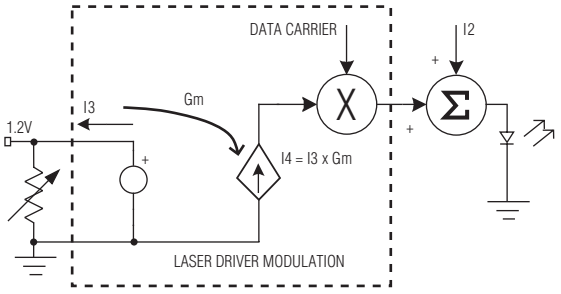

Figure 2a

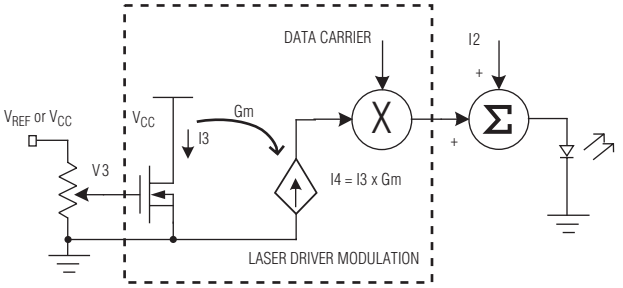

Figure 2b

Figure 2. Circuits for low-side control of laser-modulation current are similar to those for control of bias current in Figures 1a and 1b.

Less common are closed-loop modulation-control circuits. **Figures 3a** and **3b** show a resistor interface to such laser drivers.

In Figure 3a, the laser-bias current is an amplified version of the error between the current fed back from the photodiode monitor (Ifa) and a reference current (I1). As the variable resistance decreases, I1 increases. Because Ifa tracks I1, the average optical power also increases.

Figure 3b is a simplified representation of closed-loop modulation. Comparing a feedback signal derived from the photodiode current (Ifb) with a reference current (I3) produces an error that is amplified and used to modulate the data-carrier amplitude, resulting in a switched current. As resistance decreases, the peak-to-peak optical power increases. Bias current (I2) is included in Figure 3b to complete the picture.

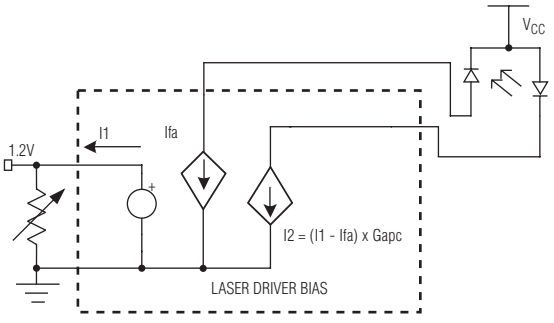

Figure 3a

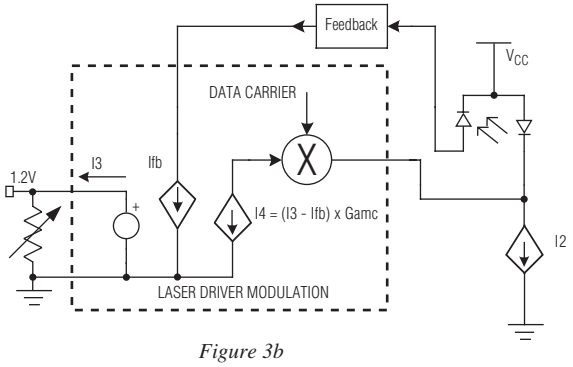

Figure 3b

Figure 3. (a) A photodiode monitor allowing closed-loop laser control can also accommodate (b) control of the modulation current.

Example: the MAX3273/DS1847 pair

To interface laser driver MAX3273 to the DS1847 digitally controlled resistor, first determine your average optical power (Pavg) and peak-to-peak optical modulation power (Pmod).

Pavg is regulated by an APC loop around the laser driver (Figure 3a), and depends directly on I1 and the photodiode's responsivity in mA/mW. The DS1847 resistor sets I1 equal to 1.2/R. Next, Pavg = I1/responsivity = 1.2/(responsivity x R).

Note the dependence of R on the photodiode characteristic in achieving the required average power. Therefore, to achieve reasonable design yields, it is recommended that the designer know the statistical distribution of this parameter as well as its temperature dependence. For example, A DFB laser (SLT2170-LN) with Pavg = 0.4mW produces a photodiode current that ranges upward from 0.15mA, which in turn calls for <8kΩ resistance. Resistor 1 internal to the DS1847 should be used for the APC function.

Pmod is not regulated within the laser driver, and therefore runs open loop. It is controlled by a resistor that sets I3 (see Figure 2a). In turn, I3 sets the peak-to-peak modulation current, which is added to the bias current and injected into the laser. As a result, the laser-light output consists of a DC component and a pulsed component. The pulsed component (Pmod) depends on the laser quantum efficiency (η) expressed in mW/mA, the gain Gm (Figure 2a), and I3 (which equals 1.2/Rmod). Thus, Pmod = 1.2 x Gm x η/Rmod.

Again, Rmod depends on η for a given Pmod, so it is important to understand the variation of h. For a system that includes the same laser (SLT2170-LN) with Pmod = 0.6mW, Gm = 165, and η = 0.06, the required resistance is less than 20kΩ. The DS1847's resistor 0 should be used for the modulation function.

The DS1847 includes look-up tables for temperature compensation (refer to Maxim/Dallas Semiconductor Application Note 167, *Considerations for the DS1847/1848 Look-Up Tables*). Such compensation is essential for the APC and modulation controls. In APC mode the table serves to offset the temperature dependence of photodiode responsivity, which varies as much as ±1.5dB (about 40%) per the SLT2170-LN data sheet. As for modulation, the corresponding table serves primarily to offset temperature dependence of the laser efficiency η, which can vary as much as ±3dB (a factor of 2).

An added benefit of look-up tables is their help in compensating the temperature dependence of laser-driver gain, resistor value, and other parameters in the application. The DS1847 resistor value is characterized at various temperatures in the Dallas factory. The result fits into an equation, whose coefficients are stored in registers for use during calibration at the customer site (refer to Application Note 167).

To illustrate some of the concepts described in the previous paragraph, **Figures 4a**, **4b**, and **4c** show typical characteristics in lasers and photodiodes after they are temperature compensated with look-up tables.

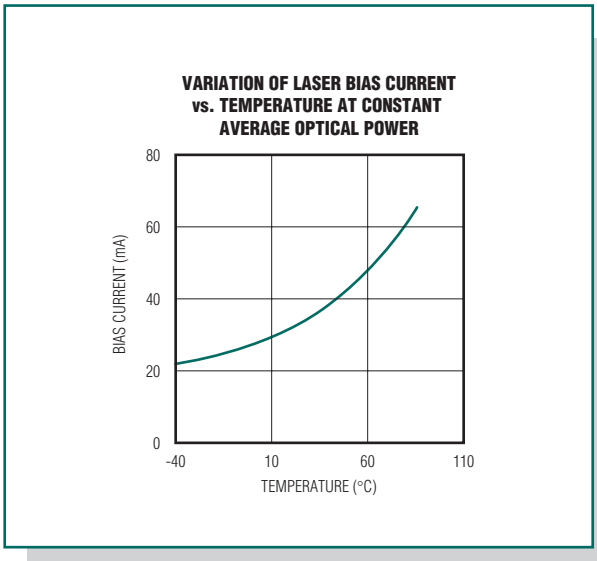

Figure 4a. A laser bias current variation is implemented with a look-up table if an open-loop operation such as Figure 1a is used.

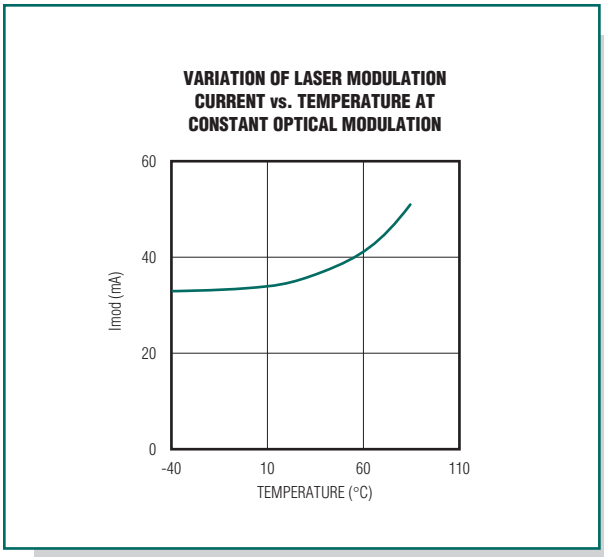

Figure 4b. A peak-to-peak laser modulation current variation is implemented with a look-up table if an open-loop operation, such as Figure 2a, is used.

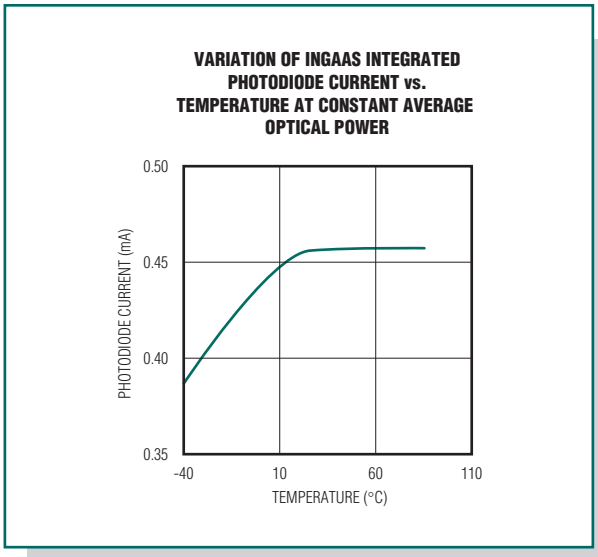

Figure 4c. An integrated photodiode current variation is implemented with a look-up table if a closed-loop operation (APC), such as Figure 3a, is used.

Frequency under-sampling in coulomb-counting applications

Many methods are available to measure current, whether pulsed or not, but the array of choices narrows for the purpose of tracking net current flow into and out of a battery. Nearly all battery-powered portable equipment uses a very low value series resistance as a current sensor, then converts the series voltage drop to a digital quantity. Several analog-to-digital converter (ADC) methods are used in commercial coulomb-counting products today. Products using delta-sigma, and especially voltage-to-frequency converter (VFC) methods, became popular because of claims about integrating high-frequency signal components. These claims imply that discrete sampling ADC methods are not accurate. However, an understanding of sampling theory, the current waveforms of specific applications, and test data explain why, and show that ADC sampling can serve as an accurate coulomb counter.

Coulomb counting in portable equipment

First, it is important to understand that the purpose of the measurement system in a coulomb-counting application is to accurately track the net flow of current into and out of the battery. Accurate measurement of net current flow is essential to the fuel-gauging goal of maintaining an accurate count of the charge stored in the battery. Although current waveforms in portable equipment are complex, only the integral of the current waveform is of interest (i.e., no waveform reconstruction is necessary). Therefore, all frequency information can be discarded as long as an accurate count of the net charge is maintained.

A second requirement for portable applications is low impact on battery life as a consequence of adding the current measurement. One aspect of this limits the power consumed by the coulomb counter to less than 0.5mW, since the measurement system is required to operate continuously without adding significantly to the drain on the battery. Additionally, the value of the sense resistor needs to be small compared with the total series resistance of the pack to minimize I^2R losses.

The third requirement for accurate coulomb counting in most portable systems is a large dynamic range. Typically, portables operate in at least two power levels. One is a standby or low-power mode where activity is low or performed periodically. The other is a high-power level where the device performs its intended task. Usually, the high-power mode is invoked briefly between long periods of operation in the low-power mode. In mobile phones, the high- and low-power modes are termed talk and standby modes, respectively. Like mobile phones and other wireless devices, most portable products switch automatically between power modes with no method to signal the coulomb counter. This requires the current-measurement system to account for low-current levels over long periods of time as well as high-current levels over shorter periods with unpredictable switching between modes. Linearity across the dynamic range is required to accurately accumulate the current flow captured in all operational modes.

When all aspects of the application requirements are considered, the extent of the design challenge emerges. Accuracy requires integrating small currents over periods of days, as well as large currents over periods of minutes with a dynamic range of 35dB to 45dB required to capture the minimum and maximum amplitudes. The measurement system must be implemented in a very low-power circuit to conserve battery energy; however, low-power circuits are more susceptible to noise. With battery-cell and protection-circuit resistances constantly falling, so do the signal levels the coulomb counter is required to measure. Acceptable sense resistor values in the 10mΩ to 30mΩ range result in low-power mode current-sense signals in the tens of microvolts. To achieve coulomb-count accuracy in standby mode over several days, resolution and input offset errors must be less than 20µV. This is because 96mAh accumulates each day given a 25mΩ resistor and 100µV of combined resolution and input-offset error. A fully charged 650mAh battery would appear to drain completely when left disconnected for a week, or worse still, a discharged battery would appear to become fully charged.

Wireless handset current waveforms

The current waveforms found in digital wireless handsets that conform to the GSM and CDMA wireless standards exhibit the two-power mode behaviors described above. But they are particularly challenging since the power amplifier (PA) transmits in short bursts, and the PA current dominates other load components. The high-power mode of a digital handset consists of repetitive current pulses for

each transmission burst while a call is in progress. In standby, the PA is pulsed at a much lower rate to answer the periodic paging of the cell tower. Paging intervals typically range from 0.5s to 2s. Besides the pulse-rate variation, pulse amplitude varies in both talk and standby modes. This is because PA power is adjusted to correspond to receive power, which is primarily related to the distance of the handset to the cell tower.

GSM/GPRS

The GSM standard defines a 4.615ms frame consisting of eight time slots on each channel. Time slots are shared, so that each GSM handset operating on a channel uses one slot for transmit and one for receive. When a call is in progress, the PA current exhibits a pulse waveform with a 12.5% duty cycle as shown in **Figure 1**.

Typical and worst-case PA currents are 1A and 3A, respectively. Figure 1 was taken from a GSM handset indicating full signal strength during a call. The voltage across the filter capacitor is the signal presented to the ADC of the discrete-sampled device.

The GPRS standard implemented on a GSM network uses additional slots to increase the data rate. Additional slots are assigned for receive or transmit. When data are being uploaded from the handset to the network, up to four slots can transmit data under GPRS class 12. The battery current of a handset operating in GPRS class 12 would exhibit a 50% duty cycle since the PA transmits in four consecutive slots.

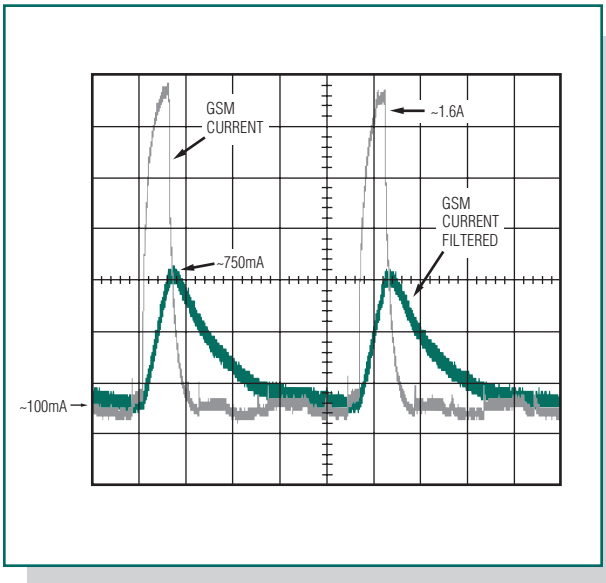

Figure 1. A GSM handset current indicates full signal strength during a voice call.

CDMA

The CDMA standard defines a 20ms frame divided into 16 power control groups. Each group has a period of 1.25ms, and various combinations of the 16 are used depending on the data rate. The PA transmitter power is varied from one 1.25ms period to the next. If the period is not used to transmit data, the power is dropped by as much as 20dB. The current waveform of a CDMA PA has a worst-case maximum amplitude of 600mA, so it is less challenging from a coulomb-counting perspective.

Theory of undersampling

While not meeting the strict definition of the intentional undersampling technique used for frequency down-conversion and waveform reconstruction, uncorrelated undersampling near the signal frequency accurately captures the average value (DC content) of a repetitive signal. By definition, the DC value of a repetitive signal does not depend on frequency or phase and, which can be seen from the Fourier series:

$$f(t) = A_0 + A_1 \sin(\omega_1 t + q_1) + A_2 \sin(\omega_2 t + q_2) + \ldots + A_n \sin(\omega_n t + q_n)$$

The average value of f(t) = A0 for all Aω, A_n, q_n, and t. As long as the sample rate is not a harmonic of the energy carrying frequencies, it is unimportant when the signal is stationary (i.e., when A0 is constant). Using a square wave as an example, the DC value represented by A0 does not change with frequency; undersampling at any frequency other than the fundamental or a multiple of its harmonics will capture a square wave of lower frequency with the same DC content.

To achieve the goal of coulomb counting, accurate measurements of the average signal value can be obtained through undersampling, even if the signal of interest exhibits low-frequency, nonrepetitive components, or distinct modes of DC content. When compared to the sample frequency, undersampling is valid even if the low-frequency components are below the Nyquist sample rate or the discrete modes persist for long periods. Consider the square-wave example and imagine the duty cycle is modulated by a signal 1/10 the sample frequency. The sampler could discard 8 of 10 samples and still faithfully reproduce the modulating signal. Next, imagine the duty cycle rotating slowly but randomly through three discrete modes: 50% to 10% to 1%. The DC value of each mode is different and important, but as long as each mode persists long enough compared to the sample rate, the signal can

be considered stationary during each mode. In both cases, the DC content can be accurately measured.

While timebase errors are important for undersampling techniques applied to both waveform reconstruction and coulomb counting, waveform recovery using intentional undersampling is sensitive to distortion due to sample-to-sample jitter. A high-quality timebase with low drift and low jitter is critical to the performance of such systems. However, since frequency and phase information are unimportant in coulomb counting, a timebase that maintains an accurate interval from sample-to-sample is not required, but the average frequency must be stable and the net clock jitter must have a zero mean. Also, to remain uncorrelated, the sample frequency, including worst-case drift, cannot equal the signal frequency or its harmonics. The timebase must maintain long-term frequency stability with zero mean jitter for accurate measurement of the DC content.

Test results

To illustrate the effectiveness of a discrete-sampled measurement device in a pulsed-current coulomb-counting application, the DS2761 high-precision battery lithium-ion (Li+) monitor with an internal 25mΩ sense resistor was used. The test setup utilized is shown in **Figure 2**. The experiment was performed with a 700mAh prismatic Li+ cell. An Arbin battery test system was used for charging the cell and for GSM load simulation.

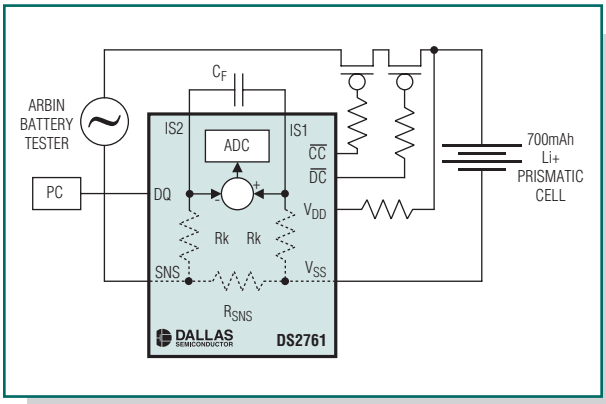

Figure 2. The effectiveness of a discrete-sampled coulomb counter in a pulsed-current application can be demonstrated in the lab using a simulated GSM or CDMA load from an Arbin battery tester.

The Arbin was programmed to perform the following pattern. The cell is fully charged by a constant current/constant voltage (CC/CV) method, then fully discharged under a continuous GSM load. It is then recharged again, and finally discharged under a DC load equivalent to the average of the GSM load. A PC recorded DS2761 data (real-time current, temperature, cell voltage,

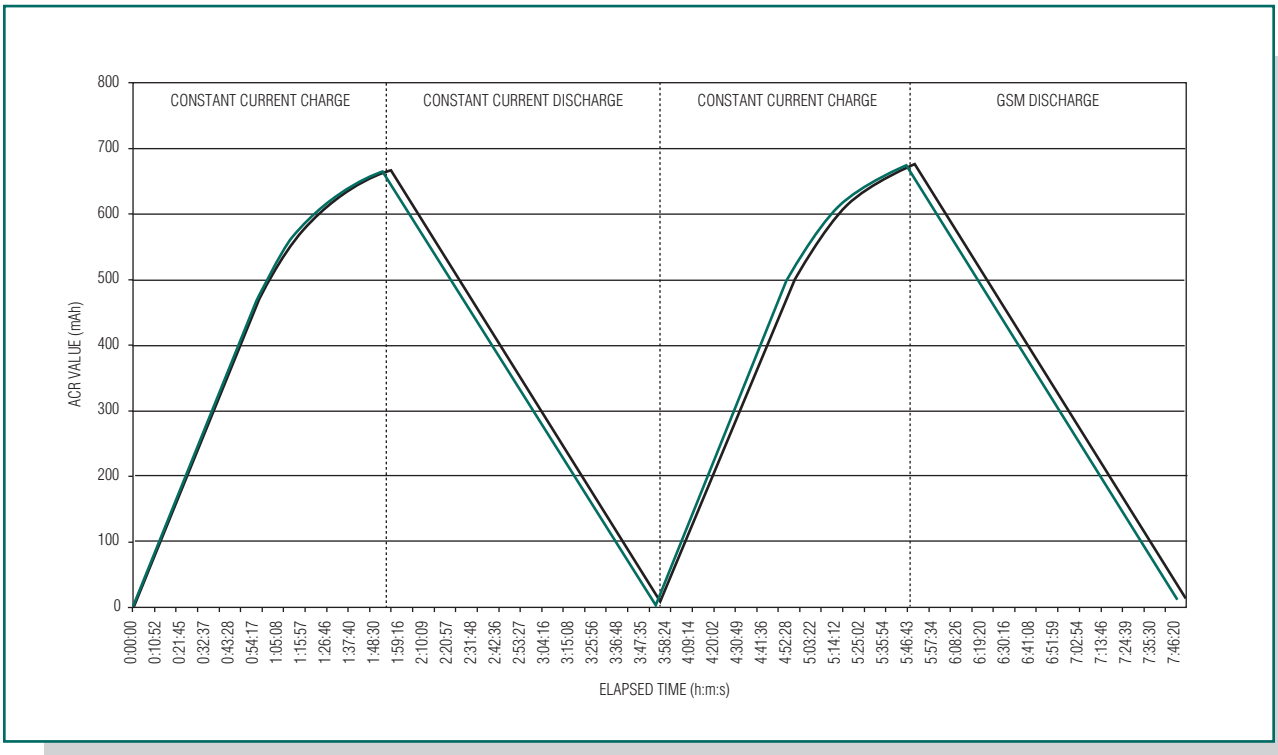

Figure 3. The two waveforms illustrate the DS2761 ACR valve with and without the prefilter capacitor.

Table 1. ACR value at charge and discharge endpoints

ENDPOINT	FILTERED		UNFILTERED		FILTER DELTA	
	ELAPSED TIME	ACR	ELAPSED TIME	ACR	ELAPSED TIME	ACR
CC/CV Charge	1:51:27	664.95	1:54:24	665.69	0:02:57	0.11%
CC Discharge	2:01:20	657.11	2:01:08	656.62	0:00:12	-0.07%
CC/CV Charge	1:52:13	664.71	1:53:12	665.69	0:00:59	0.14%
GSM Discharge	2:00:57	660.54	2:01:12	659.69	0:00:19	-0.18%
CC/GSM Delta	**0.32%**	**-0.49%**	**0.11%**	**-0.39%**		

It is beyond the scope of this article to discuss gain, offset, resolution, charge efficiency errors, and other factors that contribute to the ACR not always returning to the same point. This will be addressed for discrete-sampled and other measurement topologies (sigma-delta, VFC) in a future edition of the *Maxim/Dallas Semiconductor Engineering Journal*. This article seeks to validate frequency undersampling in coulomb-counting applications with pulsed waveforms, so the last row of data in the table is of most interest.

and accumulated current) approximately every 5s. This profile was performed once with a prefilter capacitor (C_F = 0.1µF) and then repeated without the capacitor to investigate the effect of the prefilter lowering the amplitude of the waveform presented to the ADC, as shown in Figure 1.

For the charge cycle, the cell was charged at 0.7C (490mA) constant current until the cell voltage reached 4.2V. The cell was then topped off under constant voltage at 4.2V until the charge current dropped below 0.1C. The GSM load was simulated with a 2.0A peak current for 550µs and a period of 4.6ms (12% duty cycle). The current between pulses was programmed to 100mA. Thus, an average current of 327mA resulted from the GSM waveform. The cell was considered fully discharged when its voltage reached 3.0V.

Results from the experiment are presented in two ways. **Figure 3** displays the DS2761 accumulated current register (ACR) value as a function of time over the charge, CC discharge, and GSM discharge cycles. The two waveforms represent the ACR with and without the prefilter capacitor. In this experiment, no correction was made to the ACR at the end points of each charge/discharge cycle, although this is commonly done in practice by fuel-gauging algorithms (refer to Application Note 131, *Lithium-Ion Cell Fuel Gauging with Dallas Semiconductor Devices*).

If there were no input offset or resolution errors and if the cell's charging efficiency was 100%, one would expect the value of the ACR to return to zero every time the cell was fully discharged. In practice, measurement errors and cell-charge inefficiencies contribute to the errors that appear in the ACR value at each charge/discharge endpoint shown in **Table 1**.

With the prefilter, the time difference in discharging a full cell under pulsed-GSM load and a DC load equal to the average of the GSM waveform was 23s, or 0.32% of the total discharge time under DC load. The difference between what the ACR decremented under these two loads was 3.43mAh, or 0.49%, of the rated cell capacity. The discharge time and ACR deltas were actually lower for the case with no prefilter, at 0.11% and 0.39%, respectively.

Table 1 illustrates the deviation at the endpoints, but the cycle times differed depending upon the discharge profile and whether a filter capacitor was used. **Figure 4** expands on that by highlighting the ACR difference between the GSM and CC discharge cycles as a function of time, with and without a filter capacitor. This curve is generated from the discharge cycles shown in Figure 3, but with offsets in the ACR data removed so they are equal at the start of each discharge. Doing so allows us to display the ACR delta between GSM and CC discharges, while zeroing out offsets from previous cycles.

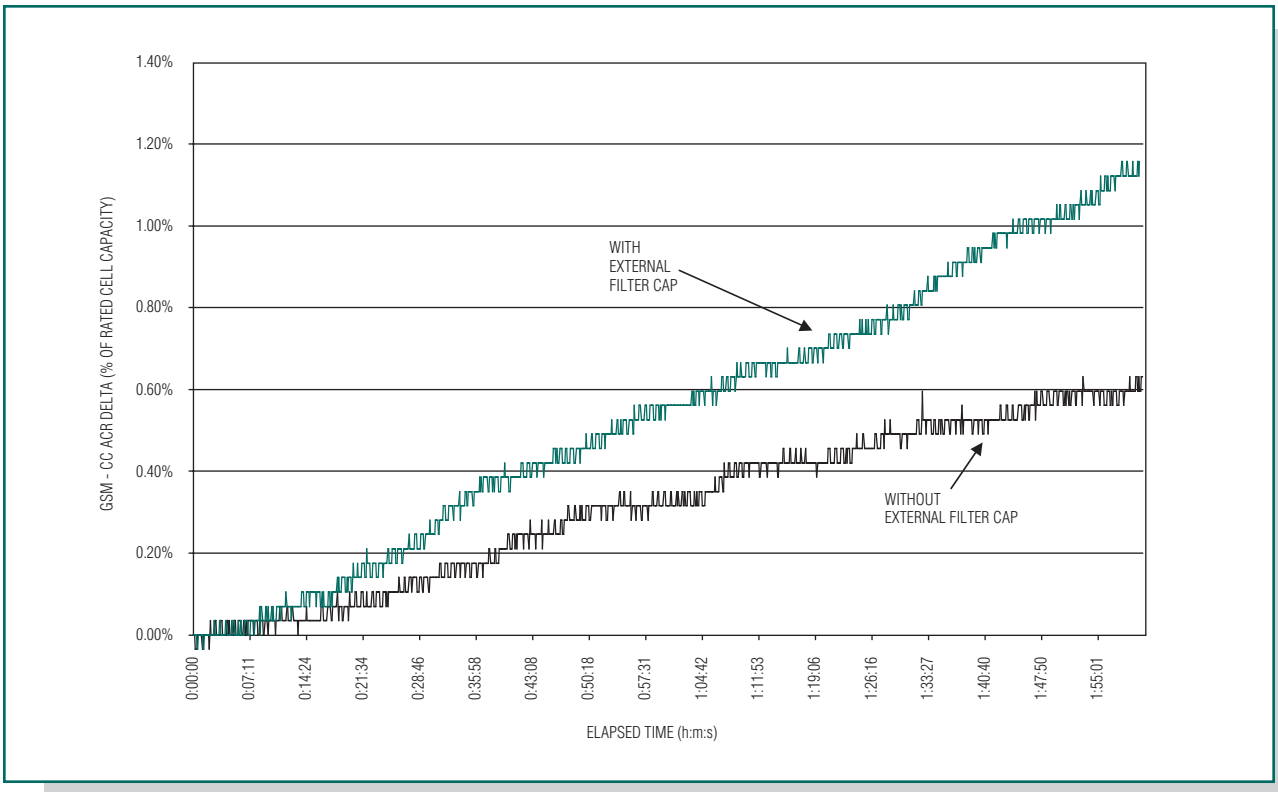

Figure 4. The difference in measured ACR between one GSM and one constant current discharge illustrates the deviation at the endpoints.

Consistent with the endpoint data, the presence of the filter cap does not offer a benefit, but appears to degrade performance under the GSM load. Although the prefilter integrates energy at high frequencies and reduces the sample rate requirements, its main purpose is to expand the dynamic range of the ADC under a pulsed load. A 1.6A pulse at 12% duty cycle (750mA filtered peak from Figure 1) does not exceed the 1.8A dynamic range limit of the DS2761, and thus the filter offers no benefit. In applications with higher current or larger duty cycles where the unfiltered signal may saturate the ADC, the benefit of the prefilter becomes more evident.

Conclusion

At first glance, a discrete ADC sampling that samples near the frequency of interest may not appear applicable. There is a temptation to apply the Nyquist sampling criterion generally. However, this study reviewed the application requirements and the criteria required to apply undersampling techniques, and in particular those relevant for measuring a signal's average value. The concept of uncorrelated undersampling near the signal frequency was shown qualitatively as an accurate method to capture DC content of a repetitive signal. Further, the frequency undersampling technique was quantitatively supported by measurements taken during charge and discharge (DC and pulse current) cycles using the DS2761 high-precision Li+ battery monitor. The data show that the deviation between the coulomb count under a DC discharge and a GSM load discharge is less than 1% of the rated cell capacity.

Exploiting the versatility of the DS4000 digitally controlled, temperature-compensated crystal oscillator in GPS applications

Global Positioning Systems (GPS) are used in a variety of applications. A network of satellites (up to 27) that fly in a non-geostationary, low-earth orbit and span the earth enables these systems. A minimum of four satellites must be acquired for the GPS receiver to provide positional information. These satellites broadcast or transmit long sequence codes or digital patterns called pseudorandom codes. Using factors such as the known pseudorandom codes from the satellites, the speed of light, and look-up tables that hold satellite position, GPS receivers can determine the travel time of the satellite signal and convert this travel time to distance. With multiple (>4) satellites, triangulation routines are used to determine the position of the GPS receiver, thus providing the user's location.

The applications for GPS receivers range from the general-purpose hand-held devices for individual navigation and mapping to marine, aviation, surveying, and timing synchronization in telecommunication networks. Each application requires different characteristics from the receiver. For example, in a general-purpose hand-held application, the receiver will make use of four or more of the received satellites' signals and convert this information into positional information that can be tied to map databases for terrestrial location. In marine or aviation applications, dynamic positional data taken from the received satellite signal can be directed into the ship's or aircraft's onboard navigational system for real-time positioning and direction. Another important feature and use of GPS is to provide an extremely accurate time reference for synchronization in telecommunications networks, calibration of test and measurement equipment, synchronization of astronomical observations and observatories, seismology stations, or fault recorders for electric utility grids. For synchronization and timing, the phase of the satellite's signal is more important than the data carried in that signal.

In applications where timing synchronization is the priority, the phase differences of the transmitted signals are most important. In telecommunication networks, GPS synchronization engines provide end-to-end timing of these types of networks. Most important to this need is the requirement for quality of service in operating the network for voice, video, or the time-critical transfer of data.

An accurate frequency reference is critical for synchronization and timing requirements. The most accurate timing references are generated from atomic clocks. To that end, the international-standard definition of time and frequency is based on the cesium atom. An accurate frequency is generated by a cesium-beam standard. What makes the GPS satellite system accurate enough for network synchronization? Each GPS satellite has a cesium-based timing source. These very precise clocks keep accurate time to within three nanoseconds per day. Accurate timing can then be transferred by radio wave to GPS receivers.

To keep accurate timing, the GPS receiver has an internal local oscillator such as rubidium, an oven-controlled crystal oscillator (OCXO), or even a temperature-compensated crystal oscillator (TCXO) that serves as a disciplined time source to maintain accuracy and stability over both short and long periods. Because the GPS satellites are available worldwide, the use of GPSs enable synchronization of telecommunications networks in a feasible, accurate, and economical manner. A host of suppliers provide GPS-enabled equipment to support timing synchronization of telecommunication networks, basestations, and other time-critical applications.

Examining the GPS receiver

A typical GPS receiver application will have functional blocks as shown in **Figure 1**. Included in these blocks will be the radio frequency (RF) section, GPS signal processor, and a host processor. The RF section will include the GPS antenna, an RF filter, and a GPS RF front-end. The RF section collects satellite signals,

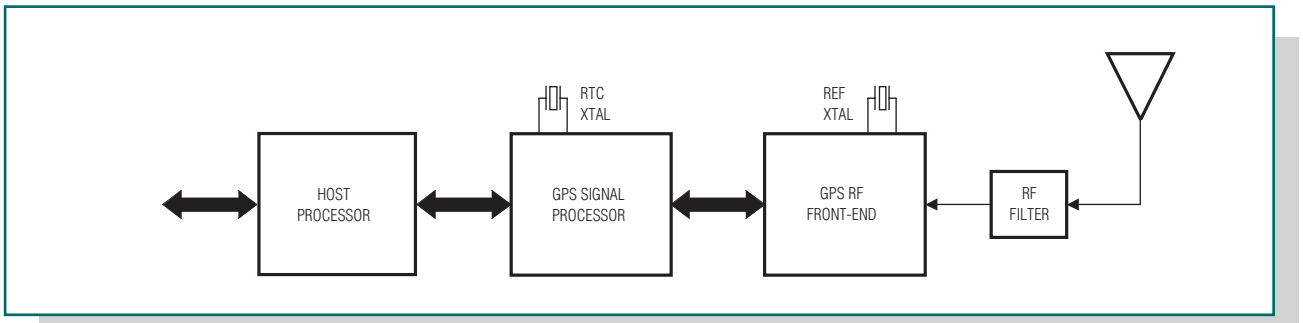

Figure 1. A typical GPS receiver system will include the RF section, a GPS signal processor, and a host processor.

stripping the pseudorandom code from the carrier frequencies and passing it to the GPS signal processor. In most receivers developed today, these front-ends plus GPS signal processors can simultaneously process 4 to 12 satellite signals in parallel. The ability to parallel process these signals provides increased precision in positional data and reduced time to provide that data. The host processor provides this data to the user either through a GUI, display screen, or other operating system conduits, depending on the application requirement.

Also shown in Figure 1 are two oscillator sources in the block diagram, which include the REF crystal or oscillator and the real-time clock (RTC) crystal. The REF crystal or oscillator can be imprecise or extremely accurate depending on the use of the receiver. The frequency requirements of this oscillator depend on the GPS front-end, application-specific standard product (ASSP) used. Values typically range from 13MHz to 30MHz, depending on the manufacturer. In applications that use the GPS receiver as a precise timing reference, this REF oscillator could be a rubidium source, an OCXO, or even a TCXO. The host processor in this case would be used to correct any timing slips between the satellite and the receiver.

The RTC crystal provides real-time clock information to acquisition routines to acquire the different satellites in the 27-satellite constellation. With the look-up table on satellite positional information, the RTC aids in providing a starting point for locking all visible satellites.

Introducing the DS4000

With the introduction of the DS4000 digitally controlled TCXO, new control methods for addressing the correction of the REF oscillator can be addressed. The DS4000 provides precise oscillator requirements and unique features not available in many TCXOs in the marketplace. First, the DS4000 is factory calibrated for accuracy to within ±1ppm. Additionally, the device provides digital pullability with a pull range of ±6ppm and a typical resolution of less than 0.1ppm. **Figure 2** is a block diagram of the DS4000. The device is controlled through a 2-wire serial port. In this manner, digital codes manage pullability/ accuracy through the use of a microcontroller. System routines can be devised that continuously manage the device's accuracy. In many older TCXO designs, this requirement could only be fulfilled through manual tuning or through a secondary voltage control. The digital tuning capability of the DS4000 provides automated calibration during manufacturing and also recalibration while equipment is in the field.

The device also has a second frequency output, F2, which is a fraction of the fundamental frequency, F1. F2 can be programmed to provide 1/256th to 255/256th of the F1 frequency. Again, this programmability is achieved through the 2-wire control port. The DS4000's fundamental frequency options range from 10MHz to

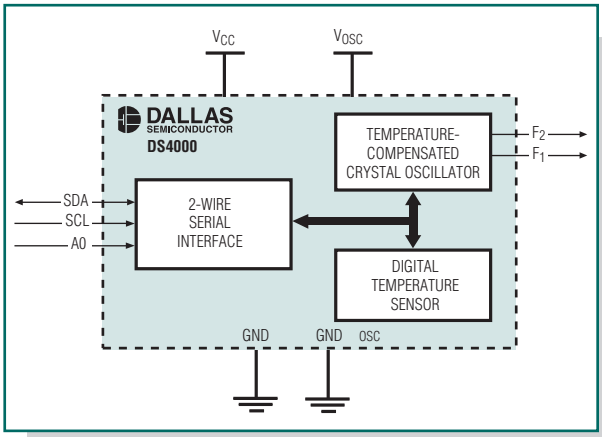

Figure 2. This block diagram of the DS4000 illustrates digital access to frequency pullability, frequency output, and temperature sensing.

20MHz. The F2 output follows F1 in accuracy and is also accurate to within ±1ppm.

Because the DS4000 uses Dallas Semiconductor's patented digital temperature-sensing technology, the device can also be a temperature sensor in the application. The accuracy of the temperature sensor is within ±2°C. The device maintains its frequency accuracy (±1ppm) over the full industrial temperature range of -40°C to +85°C.

Using the DS4000 in a GPS application

Because the DS4000 is so versatile, it could be used to provide the disciplined oscillator for the REF crystal (XTAL) in the GPS application as well as provide the 32kHz input to the RTC XTAL for the GPS signal processor or host processor in some cases. **Figure 3** illustrates the DS4000 fulfilling the role of both the REF and RTC XTALs in the GPS receiver block diagram.

Certain assumptions are made about the fundamental frequency used in Figure 3's block diagram. First, it is assumed that the REF XTAL input to the GPS front-end can use a 16.384MHz frequency input. If this is true, the DS4000 can generate a 32.768kHz frequency on the F2 output for the RTC requirement to the GPS signal processor. Through the 2-wire interface, the host processor would control the pullability, F2 frequency out, and temperature sensing if needed.

Summary

GPS applications represent one of many applications where highly accurate timing sources are used. The flexibility of the DS4000 makes it ideal where accurate timing and device control are paramount. Typically, TCXOs or OCXOs that allow frequency tuning require that tuning be done manually, or with the provisions of an externally controlled voltage. The drawbacks of such tuning strategies include the need for human intervention in the case of a manually tuned TCXO or OCXO. When tuning with an externally controlled voltage, the designer must ensure that the control voltage is stable so it does not affect the output characteristic of the oscillator. The DS4000 removes both uncertainties in tuning because it requires only a digital code to be transmitted to it for changing or pulling the fundamental frequency.

Additionally, since the DS4000 provides two frequency outputs (F1 and F2), one of which is programmable, the user can now eliminate a second oscillator if F2 (or the second required frequency) is related to F1 through an integer division. Finally, the DS4000 contributes to automated calibration flows for equipment with its digitally controlled interface. This aspect of the device eliminates the need for equipment to be periodically recalibrated over the life of the product.

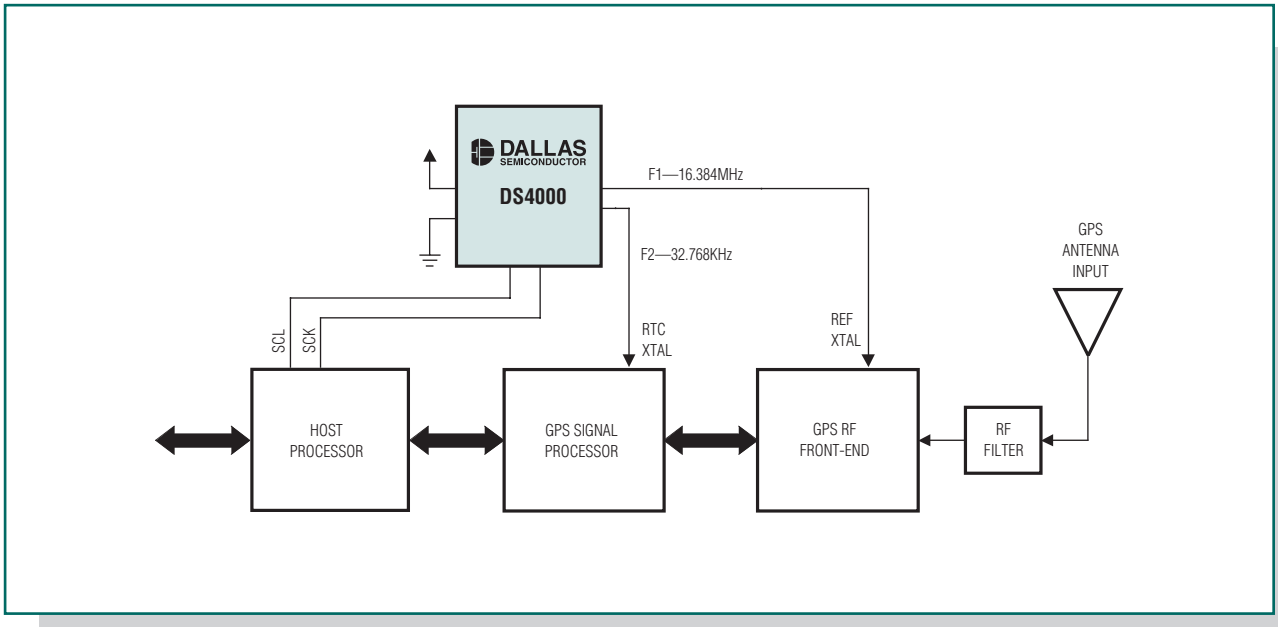

Figure 3. The DS4000 fulfills the role of both the REF and RTC XTALs in a typical GPS receiver application.

DS2155 and DS2156 universal line interface circuits

In today's telecommunications industry, it is often necessary to design a single piece of equipment that operates with the existing telecommunications systems used throughout the world. These designs must interface with the T1 standard used in North America, the J1 standard used in Japan, and the E1 standard used throughout the rest of the world. To help manufacturers produce a design of this nature, Dallas Semiconductor introduced a line of T1/E1/J1 combination single-chip transceivers (SCTs). The DS2155 and DS2156 SCTs provide a single hardware platform for T1/E1/J1 communications. The digital section of these devices contains the framer/formatter, clock synthesizer, jitter attenuation circuit, HDLC controller, and system interface. The analog section of these devices that connects to the network interface contains a complete long- and short-haul interface with transmit-wave shaping and receive-clock and data recovery. These devices can be reconfigured with minimal effort and therefore provide an easy solution for interfacing to telecommunications systems throughout the world.

While these devices provide a common design interface for each of the transmission systems, physical differences exist in both the cable and connector types used in each system. **Table 1** shows a list of the transmission systems along with the cable type, cable impedance, and the possible connector types.

The most common physical connection between these systems is made using the RJ-48 connector and a balanced twisted-pair cable. Balanced twisted-pair cable can also use the Bantam or Siemens 3-pin connectors but they are not as common as the RJ-48. Another popular connection used in E1 systems is made with the BNC connector and single-ended coaxial cable. Because of the electrical and physical differences between the balanced twisted-pair cable with an RJ-48 and the single-ended coaxial cable with a BNC, it is often difficult to build a system to support both interfaces. The interface-circuit design usually requires either use of two transformers in series or a special transformer with a split secondary winding. Since the use of two transformers increases cost, complexity, and board space, this article focuses on the alternative single transformer solution.

Circuit description

The network interface in **Figure 1** is built around the Pulse Engineering TX1099 transformer (see parts list in **Table 2**). This transformer is a 16-pin surface-mount dual transformer. Each transformer in the package contains a split secondary winding. The transformer turn ratio is 1CT:1:0.8 and can be thought of as having two sections for the interface. The 1CT:1 section is used in the balanced twisted-pair cable connections and the 1CT:0.8 section is used in the single-ended coaxial cable connections. This circuit also contains the necessary components for secondary overvoltage protection. The balanced twisted-pair interface has longitudinal-type protection while the single-ended coaxial has metallic-type protection.

The receive side of the DS2155 and DS2156 devices normally requires the use of a 1:1 transformer. With the 1:1 transformer, the matching resistance between the RTIP and RRING pins is simply the impedance of the line (i.e., for a 100Ω balanced twisted-pair cable the resistance between RTIP and RRING is exactly 100Ω). To ease

Table 1. T1/E1/J1 systems overview

SYSTEM TYPE	CABLE TYPE	CONNECTOR TYPE
T1	100Ω balanced twisted-pair cable	RJ-48 or Bantam connector
J1	110Ω balanced twisted-pair cable	RJ-48 or Bantam connector
E1	120Ω balanced twisted-pair cable	RJ-48 or Siemens 3-pin connector
E1	75Ω single-ended coaxial cable	BNC connector

board design and layout, Dallas Semiconductor created an internal impedance-matching circuit to terminate the cable at either 75Ω, 100Ω, or 120Ω. To take advantage of this feature, the network interface must be terminated externally with 120Ω between RTIP and RRING. Changing the impedance is then performed in software using line-interface control registers. In Figure 1, the balanced twisted-pair interface uses the 1CT:1 section of the transformer and requires no modification. However, the single-ended coaxial cable interface uses the 1CT:0.8 section. To properly match the 75Ω line impedance, the ratio of the coil winding must be considered. Using the equation below, the exact termination resistance between RTIP and RRING for 75Ω would equal 117Ω. If 120Ω is chosen for the termination resistance the resulting impedance seen by the line will be 76.8Ω.

$$\text{Termination} \times (0.8)^2 = 75\Omega$$

$$120\Omega \times (0.8)^2 = 76.8\Omega$$

This value is close enough to the ideal 75Ω to properly terminate the line. Therefore, the software should configure the device-receive termination for 120Ω whenever E1 communication is enabled.

The transmit side of the DS2155 and DS2156 devices normally requires use of a 1:2 transformer. To achieve the necessary primary-to-secondary winding ratio, the center tap of the TX1099 primary side is connected to one of the outputs (TRING is chosen in Figure 1). The transformer is now a 1:2:1.6 with the 1:2 section connected to the balanced twisted-pair cable and the 1:1.6 section connected to the single-ended coaxial cable. Using the circuit in Figure 1, the pulse amplitude and template can be modified through software alone. As with the receive side, the balanced twisted-pair interface requires no design changes because it meets the required transformer specifications. Since the single-ended coaxial cable interface uses the 1:1.6 section, the resulting pulse amplitude will not meet specifications when the device is set for 75Ω E1 transmission. Under normal operation, the pulse amplitude is doubled by the 1:2 transformer, but in this case it is only multiplied by 1.6, resulting in a pulse that is only 80% of the ideal amplitude. To create the necessary pulse amplitude in the cable, the line build-out is set for 120Ω. The 120Ω line build-out setting creates a nominal 1.5V pulse into the primary winding of the transformer that produces a 2.4V pulse at the cable.

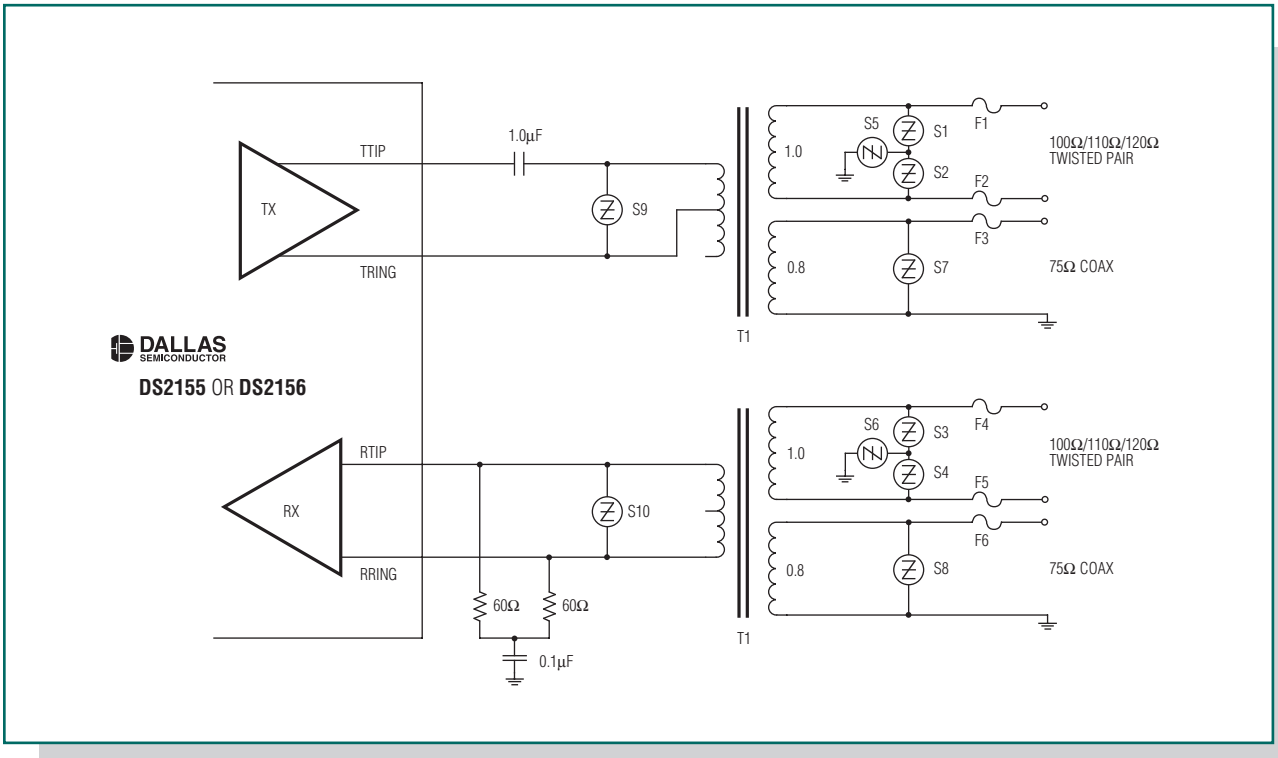

Figure 1. The DS2155 and DS2156 SCTs provide a single hardware platform for T2/E3/T1 communications.

Table 2. Dual connector interface parts list

NAME	DESCRIPTION	PART NUMBER	SOURCE
F1 to F6	1.25A slow-blow fuse	F1250T	Teccor Electronics
S1 to S4	40V transient suppressor	P0300SC	Teccor Electronics
S5, S6	220V max transient suppressor	P1800SD	Teccor Electronics
S7, S8	77V max transient suppressor	P0640SC	Teccor Electronics
S9, S10	25V max transient suppressor	P0080SA	Teccor Electronics
T1	Transformer dual SMT 1CT:1:0.8	TX1099	Pulse Electronics

$$1.5V_{OP} \times 1.6 = 2.4V_{OP}$$

This value is within the $2.37V_{OP}$ ±10% peak voltage for E1 75Ω transmission and will meet the necessary pulse-template requirements. Therefore, the software should configure the device transmit line build-out for 120Ω when E1 communication is enabled. Further details on the receive and transmit line interfaces can be found in the DS2155 and DS2156 data sheets. Alternative overvoltage protection methods, as well as how to prevent ground loops in the 75Ω single-ended coaxial connector are covered in more detail in Application Note 324, *T1/E1 Network Interface Design*, found on the Maxim-ic.com website.

Advanced rechargeable lithium battery pack solution

With the addition of the DS2770 and DS2720, it is now possible to design an affordable cell pack that supports charge control, power control, fuel gauging, cell protection, time keeping, and pack identification. The circuit shown in **Figure 1** accomplishes all of this by replacing an existing protection or protection/charge-control circuit in a cell pack.

The circuit

In Figure 1, the DS2720 is a protector for the cell, the DS2415 is a real-time clock (RTC), and the DS2770 is a charge controller/fuel gauge. All three devices share a common ground, supply, and communication line. All external capacitors and resistors shown are for signal filtering and ESD protection. The host device is powered from the PACK+ and PACK- pins on the left-hand side of the circuit. Communication to the pack takes place over the standard 1-Wire® interface labeled as data. The optional PS connection is an active-low pack-enable input designed to be connected to the system's on/off switch. The charge-source pin can handle an input of up to 15V that is current limited to the charge rating of the cell. The entire circuit draws less than 100µA typical when in active mode, and less than 20µA typical when the pack is disconnected.

Protection features

The DS2720, located in the middle of Figure 1, provides all the safety features required for a single Li+ or lithium polymer cell circuit through the use of external N-FETs. The cell is protected from overcharging, excessive depletion, high discharge currents, and high temperatures. The DS2720 has a trickle-charge feature allowing a severely depleted cell to be recovered by using the standard system charger. The host software determines what condition caused the fault and reports it.

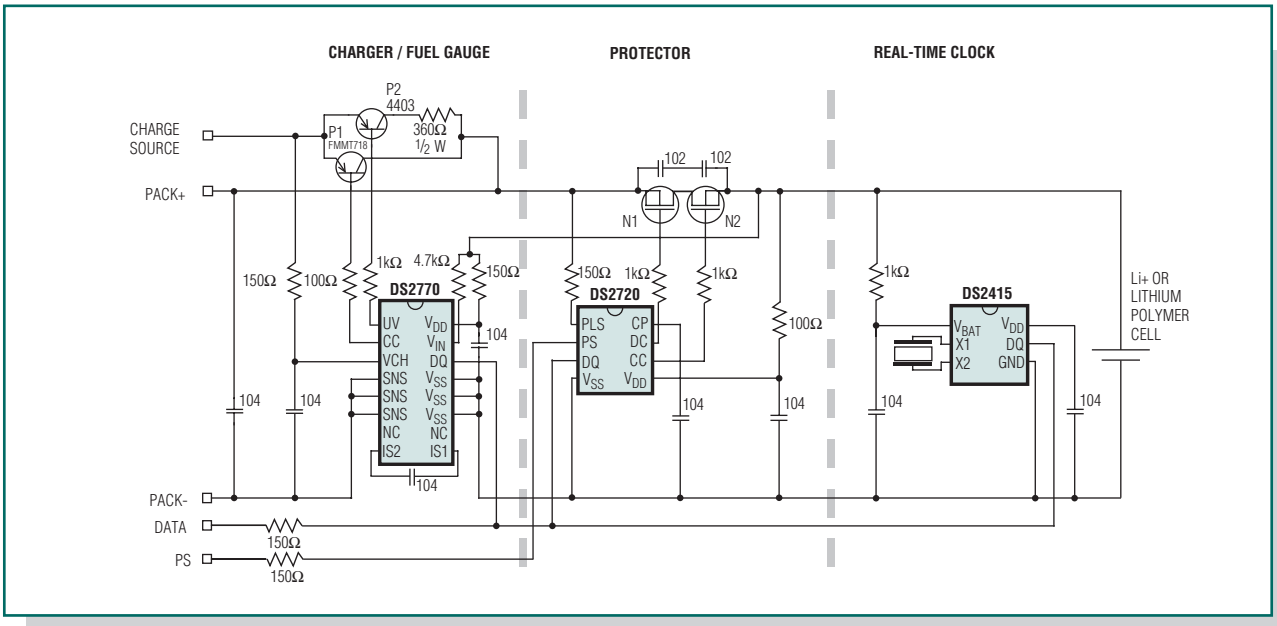

Figure 1. An existing protection or protection/charge-control circuit can be replaced by an affordable cellpack consisting of the DS2770, DS2720, and DS2415.

1-Wire is a registered trademark of Dallas Semiconductor.

Note that the protection FETs are mounted on the high side of the circuit between the host/charge source and the positive terminal of the battery, as shown in Figure 1. It is preferable to power the DS2770 and DS2415 directly from the battery. This ensures that their data will be maintained during a protection fault or when the pack is in sleep mode, the FETs are disabled, and data would otherwise be lost. It is possible to do this without violating protection rules because high-side FETs block any possible secondary charge path through the communication lines that would be a concern with low-side FETs.

Charger

One function of the DS2770 controls cell charging using a simple current-limited power source. It performs this feature independent of cell characteristics such as manufacturer or capacity. By controlling external PNP transistors (P1 and P2 in Figure 1) the DS2770 charges Li+ or lithium polymer-based packs with constant current up to a factory-set limit of either 4.1V or 4.2V. It then pulse charges to top off the cell. The DS2770 provides a secondary charge termination if the cell temperature exceeds +50°C or user-defined maximum charge-time elapses. To initiate charging, just attach a current-limited supply (up to 15V) to the charge source pad (Figure 1).

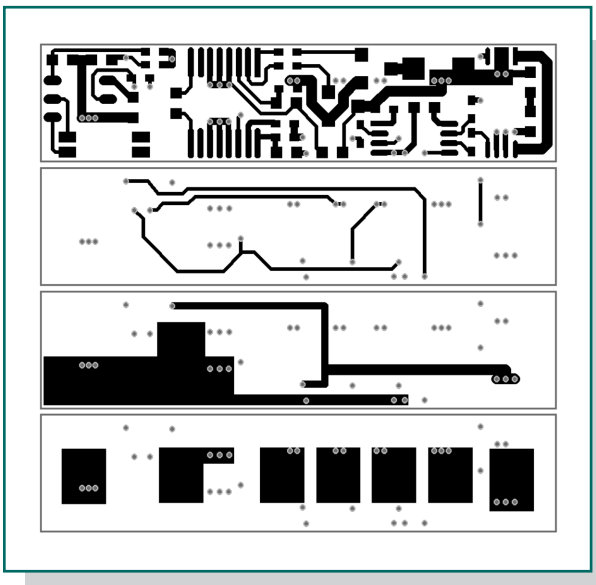

Figure 2. This circuit can be implemented in an 8.1mm x 35.5mm layer board.

Fuel gauge

The DS2770 also operates as a highly accurate fuel gauge. Current is measured through an internal 25mΩ sense resistor down to a resolution of 62.5µA with a dynamic range of ±2A average current (the input filter allows current spikes much higher than 2A to be registered in the current accumulator). The DS2770 can easily track discharge current in GSM/CDMA applications, and its internal auto compensation maintains measurement accuracy over the entire operating range of the device. Real-time measurements of accumulated current, voltage, and temperature, combined with cell characterization data stored in the DS2770's EEPROM, allow a system processor to run an accurate fuel gauge algorithm while consuming few system resources. Also, because the DS2770 is powered directly from the battery, coulomb-count information is not lost when the battery pack is removed or if power is lost due to a protection fault.

Real-time clock

The DS2415 provides an RTC accurate to two minutes per month for the host system. This requires a 32kHz, 6pF external crystal attached to the X1 and X2 pins. Because the DS2415 is powered directly from the battery, this architecture has a significant advantage over other systems. By locating the clock on the inside of the protection FETs, the system is guaranteed a clock that will maintain proper time even when system power is lost, eliminating the need for super cap or button cell backup in the host.

Pack information

The DS2770 contains 40 bytes of user-accessible EEPROM and the DS2720 has an additional eight bytes. The pack manufacturer should use this space to store relevant pack information such as cell chemistry, assembly date, cell characterization information for fuel gauging. Once written to, the EEPROM can be permanently locked ensuring data integrity even through power loss and ESD events. In addition, each chip has a unique 64-bit serial number that can be used for pack identification.